

Nucleon-nucleon scattering in a chiral constituent quark model

D. Bartz* and Fl. Stancu†

Université de Liège, Institut de Physique B5, Sart Tilman, B-4000 Liège 1, Belgium

(November 7, 2018)

Abstract

We study the nucleon-nucleon interaction in a chiral constituent quark model by using the resonating group method, convenient for treating the interaction between composite particles. The calculated phase shifts for the 3S_1 and 1S_0 channels show the presence of a strong repulsive core due to the combined effect of the quark interchange and the spin-flavour structure of the effective quark-quark interaction. Such a symmetry structure stems from the pseudoscalar meson exchange between the quarks and is a consequence of the spontaneous breaking of the chiral symmetry. We perform single and coupled channel calculations and show the role of coupling of the $\Delta\Delta$ and hidden color CC channels on the behaviour of the phase shifts.

Typeset using REVTEX

PACS numbers: 24.85.+p, 21.30.-x, 13.75.Cs

I. INTRODUCTION

Many studies have been devoted so far to the understanding of the nucleon-nucleon (NN) interaction starting from models which have been considered to be successful in baryon spectroscopy. Here we refer to nonrelativistic quark models in the framework of which calculations of scattering phase shifts can be made quantitatively. We can roughly divide

*e-mail : d.bartz@ulg.ac.be

†e-mail: fstancu@ulg.ac.be

these models into three categories. In the first category we consider models based on one-gluon exchange (OGE) between quarks. They explain the short-range repulsion of the NN potential as due to the chromomagnetic spin-spin part of OGE, combined with quark interchanges between $3q$ clusters (for a review see e.g. [1–4]). In addition, the long-range part is obtained from the one-pion exchange potential acting directly between two nucleons and the medium-range part is introduced phenomenologically as a local central potential [5].

There is a second category, of hybrid models [6–8], where in addition to OGE, quarks belonging to different clusters interact also via pseudoscalar and scalar meson exchange. In these hybrid models the short-range repulsion is still attributed to OGE and the middle- and long-range attraction is due to meson exchanges between quarks.

Here we employ a model of the third category where the quark-quark interaction, besides the confinement, is due entirely to meson exchanges between quarks. This is the chiral constituent quark model proposed in Ref. [9] and parametrized in a nonrelativistic version in Refs. [10,11]. There are also semirelativistic versions available, see e. g. [12]. For the present status of the model we refer the reader to Ref. [13].

The origin of the model [9–13] is thought to lie in the spontaneous breaking of chiral symmetry in QCD which implies the existence of constituent quarks with a dynamical mass and Goldstone bosons (pseudoscalar mesons). According to the two-scale picture of Manohar and Georgi [14] at a distance beyond that of spontaneous chiral symmetry breaking, but within that of the confinement scale, the appropriate degrees of freedom should be the constituent quarks and the chiral meson fields. If a quark-pseudoscalar meson coupling is assumed, in a nonrelativistic limit one obtains a quark-meson vertex proportional to $\vec{\sigma} \cdot \vec{q} \lambda^F$ with $\vec{\sigma}$ the Pauli matrices, \vec{q} the momentum of the meson and λ^F the Gell-Mann flavor (F) matrices. This generates a pseudoscalar meson exchange interaction between quarks which is spin and flavor dependent.

In the following this interaction is referred to as a Goldstone boson exchange (GBE) interaction. In the coordinate space the corresponding potential contains two terms. One is a repulsive Yukawa potential tail and the other is an attractive contact δ -interaction. When

regularized [10,11] the latter generates the short range part of the quark-quark interaction. The short-range part dominates over the Yukawa part in the description of baryon spectra leading to a correct order of positive and negative parity states [15]. This interaction contains the main ingredients required in the calculation of the NN potential, and it is thus natural to study the NN problem within this model. In addition, the two-pion exchange interaction between constituent quarks reinforces the effect of the flavor-spin part of the one-meson exchange and also provides a contribution of a σ -type scalar meson exchange [16] required to describe the middle-range attraction.

The spin-flavor symmetry structure of the model [9–13], which is essential in describing the light baryon spectrum is getting support from the phenomenological analysis of $L = 1$ negative parity resonances [17]. Also $1/N_c$ QCD studies [18] have a consistent interpretation in a constituent quark model with pseudoscalar meson exchange interaction. The spontaneous chiral symmetry breaking is responsible for the absence of parity doubling in low energy hadron spectrum. In particular it explains the splitting between the negative parity state $N^*(1535)$ and the nucleon $N(939)$. The quark models, as e. g. the OGE model, which explicitly breaks chiral symmetry, fail to reproduce the $N^*(1535) - N(939)$ splitting. Recent lattice calculations, which take into account the chiral symmetry of QCD [19], were able to reproduce the above $N^* - N$ splitting. This brings new substantial support to the model [9–13].

This work is a natural extension of the previous studies [20–22]. Ref. [20] was rather exploratory about the role of a spin-flavor dependent interaction in giving rise to a repulsive core. Within the parametrization [10] of the GBE model it was found that at zero-separation between two $3q$ clusters the height of the repulsive core is 0.830 GeV and 1.356 GeV in the 3S_1 and 1S_0 channels respectively. The spin-flavor symmetry and the parametrization [10] of the GBE model favours the $| [42]_O [51]_{FS} \rangle$ state which becomes highly dominant. In a better basis [21], obtained from single-particle molecular type states, instead of cluster model states, the situation is similar, the repulsion being reduced by about 200 MeV in the 3S_1 channel and by about 400 MeV in the 1S_0 channel. This is natural because the molecular orbital

basis gives a lower bound of the expectation value of the Hamiltonian in the six-quark basis. In Ref. [22] an adiabatic nucleon-nucleon potential was calculated based on the model [10]. It was found that none of the bases, cluster or molecular, leads to an attractive pocket. An attraction was simulated by introducing a σ -meson exchange of a similar analytic structure between quarks, with that of the pseudoscalar meson exchange.

Here, instead of [10], we use the chiral constituent quark model version of Ref. [11] where the GBE interaction is parametrized in a more realistic way. The adiabatic potential calculated [22] in the Born-Oppenheimer approximation with this version possesses a small attractive pocket, in contrast to that resulting from model [10] (see Ref. [21]).

The present study is based on a dynamical approach to the NN interaction, namely the resonating group method (RGM) [23–25], which allows the calculation of both bound states and phase shifts. This method has already been used in NN studies with models of categories 1) and 2) mentioned above. So far it has been always applied to nonrelativistic models, where the wave function of the nucleon can be approximated by an s^3 configuration.

In the next section we shortly review the Hamiltonian model [11]. In Sec. III we describe the main steps of the resonating group method for bound and scattering states. The $6q$ basis formed of NN , $\Delta\Delta$ and CC (hidden color) states is introduced in subsection III C. In Sec. IV we derive the matrix elements required by the RGM method for the typical spin-flavor structure of the GBE model. In Sec. V we present the results for the phase shifts in the 3S_1 and 1S_0 channels and discuss the role of the coupled $\Delta\Delta$ and CC channels on the NN phase shifts. The last section is devoted to conclusions.

II. THE MODEL

The GBE Hamiltonian considered below has the form [11]

$$H = \sum_i m_i + \sum_{i=1} \frac{p_i^2}{2m_i} - K_G + \sum_{i < j} V_{Conf}(r_{ij}) + \sum_{i < j} V_\chi(r_{ij}) , \quad (2.1)$$

where K_G is the kinetic energy of the center of mass. The linear confining interaction is

$$V_{Conf}(r_{ij}) = -\frac{3}{8} \lambda_i^c \cdot \lambda_j^c (Cr_{ij} + V_0) , \quad (2.2)$$

and the spin-spin component of the GBE interaction in its $SU_F(3)$ form is

$$V_\chi(r_{ij}) = \left\{ \sum_{F=1}^3 V_\pi(r_{ij}) \lambda_i^F \lambda_j^F + \sum_{F=4}^7 V_K(r_{ij}) \lambda_i^F \lambda_j^F + V_\eta(r_{ij}) \lambda_i^8 \lambda_j^8 + \frac{2}{3} V_{\eta'}(r_{ij}) \right\} \vec{\sigma}_i \cdot \vec{\sigma}_j . \quad (2.3)$$

The interaction (2.3) contains $\gamma = \pi, K, \eta$, and η' meson exchange terms and $V_\gamma(r_{ij})$ is given as the sum of two distinct contributions: a Yukawa-type potential containing the mass of the exchanged meson and a short-range contribution of opposite sign, the role of which is crucial in baryon spectroscopy. For a given meson γ , the exchange potential is

$$V_\gamma(r) = \frac{g_\gamma^2}{4\pi} \frac{1}{12m_i m_j} \left\{ \mu_\gamma^2 \frac{e^{-\mu_\gamma r}}{r} - \Lambda_\gamma^2 \frac{e^{-\Lambda_\gamma r}}{r} \right\} , \quad (2.4)$$

where $\Lambda_\gamma = \Lambda_0 + \kappa \mu_\gamma$. For a system of u and d quarks only, as is the case here, the K exchange does not contribute. In the calculations below we use the parameters of Ref. [11].

These are

$$\begin{aligned} m_{u,d} &= 340 \text{ MeV} , \quad C = 0.77 \text{ fm}^{-2} , \\ \mu_\pi &= 139 \text{ MeV} , \quad \mu_\eta = 547 \text{ MeV} , \quad \mu_{\eta'} = 958 \text{ MeV} , \\ \frac{g_{\pi q}^2}{4\pi} &= \frac{g_{\eta q}^2}{4\pi} = 1.24 , \quad \frac{g_{\eta' q}^2}{4\pi} = 2.7652 , \\ \Lambda_0 &= 5.82 \text{ fm}^{-1} , \quad \kappa = 1.34 , \quad V_0 = -112 \text{ MeV} . \end{aligned} \quad (2.5)$$

As already mentioned before, the reason of using the parametrization [11], instead of [10], as in the previous work [20–22], is that it is more realistic. Its volume integral, i. e. its Fourier transform at $\vec{q} = 0$, vanishes, consistently with the quark-pseudoscalar meson vertex proportional to $\vec{\sigma} \cdot \vec{q} \lambda^F$. In addition, this interaction does not enhance the quark-quark matrix elements containing $1p$ relative motion, as it is the case with the parametrization [10]. This point has been raised in Ref. [26].

At this stage we wish to stress that the above parametrization gives a good description of baryon spectra. We do not change any parameter obtained from the fit [11]. Such a parametrization is, of course, only effective. However, irrespective of the parametrization,

the flavor-spin symmetry is essential in this model. There are also semirelativistic versions of the GBE model, as for example [12] but the application of the RGM techniques to semirelativistic six-quark Hamiltonians is certainly much more involved.

III. THE RESONATING GROUP METHOD

The resonating group method [23] is one of the well established methods used to study the interaction between two composite systems. It allows to calculate bound states energies and scattering phase shifts. It has been first applied to nuclear physics in the study of the nucleus-nucleus interaction [24,25]. Its application to baryon-baryon systems was initiated by Oka and Yazaki [27]. In a baryon-baryon system, where each baryon is a $3q$ cluster, it takes explicitly into account the quark interchange between the two interacting baryons. This comes from the assumption that the total wave function can be written as

$$\psi = \sum_{\beta} \mathcal{A} \left[\Phi_{\beta} \chi_{\beta}(\vec{R}_{AB}) \right] , \quad (3.1)$$

where β is a specific channel (here $\beta = NN$, $\Delta\Delta$ or CC), \mathcal{A} is an antisymmetrization operator defined below, Φ_{β} contains the product of internal wave functions of the interacting baryons and $\chi_{\beta}(\vec{R}_{AB})$ is the wave function of the relative motion in the channel β , depending on the relative coordinate \vec{R}_{AB} between clusters A and B .

The internal wave function of each cluster has orbital, flavor, spin and color parts. In Φ_{β} the flavor and spin are combined to give a definite total spin S and isospin I so that one has

$$\Phi_{\beta} = \left[\phi_A(\vec{\xi}_A) \phi_B(\vec{\xi}_B) \right]_{SI} , \quad (3.2)$$

where $\vec{\xi}_A = (\vec{\xi}_1, \vec{\xi}_2)$ and $\vec{\xi}_B = (\vec{\xi}_3, \vec{\xi}_4)$ are the internal coordinates of the clusters A and B :

$$\begin{aligned} \vec{\xi}_1 &= \vec{r}_1 - \vec{r}_2 , & \vec{\xi}_3 &= \vec{r}_4 - \vec{r}_5 , \\ \vec{\xi}_2 &= \frac{\vec{r}_1 + \vec{r}_2 - 2\vec{r}_3}{2} , & \vec{\xi}_4 &= \frac{\vec{r}_4 + \vec{r}_5 - 2\vec{r}_6}{2} , \\ \vec{R}_A &= \frac{\vec{r}_1 + \vec{r}_2 + \vec{r}_3}{3} , & \vec{R}_B &= \frac{\vec{r}_4 + \vec{r}_5 + \vec{r}_6}{3} . \end{aligned} \quad (3.3)$$

The functions $\phi_i(\xi_i)$, $i = A, B$ are supposed to be known (see later). They are totally antisymmetric $3q$ states in orbital, spin, flavor and color space. The color part is a $[1^3]$ singlet for N and Δ states and an octet for C states. Usually the color part of a $3q$ state is not written explicitly. The same statement remains valid for the $6q$ state which is a $[222]_C$ singlet in any channel.

The antisymmetrization operator \mathcal{A} is defined by

$$\mathcal{A} = 1 - \sum_{i=1}^3 \sum_{j=4}^6 P_{ij} , \quad (3.4)$$

where P_{ij} is the permutation operator of the quarks i and j belonging to clusters $A(1, 2, 3)$ and $B(4, 5, 6)$ respectively. It acts in the orbital, flavor, spin and color space, so it can be written as $P_{ij} = P_{ij}^o P_{ij}^f P_{ij}^\sigma P_{ij}^c$ where

$$P_{ij}^f = \frac{1}{2} \lambda_i^f \cdot \lambda_j^f + \frac{1}{3} , \quad P_{ij}^\sigma = \frac{1}{2} \vec{\sigma}_i \cdot \vec{\sigma}_j + \frac{1}{2} , \quad P_{ij}^c = \frac{1}{2} \lambda_i^c \cdot \lambda_j^c + \frac{1}{3} , \quad (3.5)$$

with $\lambda_i^{f(c)}$ the Gell-Mann matrices of $SU_F(3)$ ($SU_C(3)$) and $\vec{\sigma}_i$ the Pauli matrices.

Let us first consider the one channel case. From the variational principle one can obtain the equation determining the relative wave function $\chi(\vec{R}_{AB})$

$$\int \phi^+(\vec{\xi}_A) \phi^+(\vec{\xi}_B) (H - E) \mathcal{A}[\phi(\vec{\xi}_A) \phi(\vec{\xi}_B) \chi(\vec{R}_{AB})] d^3 \xi_A d^3 \xi_B = 0 , \quad (3.6)$$

where H is the Hamiltonian of the six-quark system. As usually (see e. g. Ref. [3]) we introduce the Hamiltonian kernel

$$\begin{aligned} \mathcal{H}(\vec{R}', \vec{R}) &= \int \phi^+(\vec{\xi}_A) \phi^+(\vec{\xi}_B) \delta(\vec{R}' - \vec{R}_{AB}) H \mathcal{A}[\phi(\vec{\xi}_A) \phi(\vec{\xi}_B) \delta(\vec{R} - \vec{R}_{AB})] d^3 \xi_A d^3 \xi_B d^3 R_{AB} \\ &= \mathcal{H}^{(d)}(\vec{R}) \delta(\vec{R} - \vec{R}') - \mathcal{H}^{(ex)}(\vec{R}', \vec{R}) , \end{aligned} \quad (3.7)$$

and the normalization kernel

$$\begin{aligned} \mathcal{N}(\vec{R}', \vec{R}) &= \int \phi^+(\vec{\xi}_A) \phi^+(\vec{\xi}_B) \delta(\vec{R}' - \vec{R}_{AB}) \mathcal{A}[\phi(\vec{\xi}_A) \phi(\vec{\xi}_B) \delta(\vec{R} - \vec{R}_{AB})] d^3 \xi_A d^3 \xi_B d^3 R_{AB} \\ &= \mathcal{N}^{(d)}(\vec{R}) \delta(\vec{R} - \vec{R}') - \mathcal{N}^{(ex)}(\vec{R}', \vec{R}) . \end{aligned} \quad (3.8)$$

The direct term of the Hamiltonian kernel, $\mathcal{H}^{(d)}(\vec{R})$, consists of the relative kinetic, the relative potential and the internal energies :

$$\mathcal{H}^{(d)}(\vec{R}) = -\frac{\nabla_R^2}{2\mu} + V_{rel}^{(d)}(\vec{R}) + H_{int} , \quad (3.9)$$

where $\mu = 3m/2$ is the reduced mass of the clusters A and B . Then Eq. (3.6) can be written as

$$\int \mathcal{L}(\vec{R}', \vec{R}) \chi(\vec{R}) d^3R = 0 , \quad (3.10)$$

where $\mathcal{L}(\vec{R}', \vec{R}) = \mathcal{H}(\vec{R}', \vec{R}) - E\mathcal{N}(\vec{R}', \vec{R})$. This is the RGM equation. Using (3.9) one can write

$$\mathcal{L}(\vec{R}', \vec{R}) = \left[-\frac{\nabla_R^2}{2\mu} + V_{rel}^{(d)}(\vec{R}) - E_{rel} \right] \delta(\vec{R} - \vec{R}') - [\mathcal{H}^{(ex)}(\vec{R}', \vec{R}) - E\mathcal{N}^{(ex)}(\vec{R}', \vec{R})] , \quad (3.11)$$

where $E_{rel} = E - H_{int}$ is the energy of the relative motion. There are two important steps in solving this equation. One is to calculate the Hamiltonian kernel (3.7) by reducing the six-body matrix elements to two-body matrix elements. This is discussed in Sec IV. Another step is the discretisation of the RGM equation. It is important both for bound and scattering states. The discretisation has been performed by using the method of Ref. [25].

A. Bound states

Here we briefly describe the discretisation procedure directly applicable to bound states. According to Ref. [25], the relative wave function $\chi(\vec{R})$ has been expanded over a finite number of Gaussians χ_i centered at \vec{R}_i ($i = 1, 2, \dots, N$) where R_i are points, here equally spaced, between the origin and some value of R depending on the range of the interaction. The expansion is

$$\chi(\vec{R}) = \sum_{i=1}^N C_i \chi_i(\vec{R}) , \quad (3.12)$$

with

$$\chi_i(\vec{R}) = g(\vec{R} - \vec{R}_i, \sqrt{2/3b}) = \left(\frac{3}{2\pi b^2} \right)^{3/4} e^{-\frac{3}{4b^2}(\vec{R} - \vec{R}_i)^2} . \quad (3.13)$$

If $g(\vec{r}, b)$ is the normalized Gaussian wave function of a quark, given by

$$g(\vec{r}, b) = \left(\frac{1}{\pi b^2}\right)^{3/4} e^{-\frac{r^2}{2b^2}}, \quad (3.14)$$

from the Jacobi transformations (3.3) it follows that the relative wave function is expanded in terms of the Gaussians (3.13) with the size parameter $\sqrt{2/3b}$. This method can be applied straightforwardly to the bound state problem. The modification necessary for treating the scattering problem will be explained later in the next subsection. The binding energy E and the expansion coefficients C_i are given by the eigenvalues and eigenvectors of the following equation :

$$\sum_{j=1}^N H_{ij} C_j = E \sum_{j=1}^N N_{ij} C_j, \quad (3.15)$$

where N is the number of Gaussians considered in (3.12). The matrices

$$H_{ij} = \int \phi^+(\vec{\xi}_A) \phi^+(\vec{\xi}_B) \chi(\vec{R}_{AB} - \vec{R}_i) H(1 - \mathcal{A}') [\phi(\vec{\xi}_A) \phi(\vec{\xi}_B) \chi(\vec{R}_{AB} - \vec{R}_j)] d^3 \xi_A d^3 \xi_B d^3 R_{AB}, \quad (3.16)$$

and

$$N_{ij} = \int \phi^+(\vec{\xi}_A) \phi^+(\vec{\xi}_B) \chi(\vec{R}_{AB} - \vec{R}_i) (1 - \mathcal{A}') [\phi(\vec{\xi}_A) \phi(\vec{\xi}_B) \chi(\vec{R}_{AB} - \vec{R}_j)] d^3 \xi_A d^3 \xi_B d^3 R_{AB} \quad (3.17)$$

are obtained from (3.7) and (3.8) respectively. By including the center of mass coordinate $(\vec{R}_A + \vec{R}_B)/2$ and transforming back to r_i ($i = 1, \dots, 6$) we get the following formulas

$$H_{ij} = \int \prod_{k=1}^3 \phi^+(\vec{r}_k - \frac{\vec{R}_i}{2}) \prod_{k'=4}^6 \phi^+(\vec{r}_{k'} + \frac{\vec{R}_i}{2}) H \mathcal{A} [\prod_{l=1}^3 \phi(\vec{r}_l - \frac{\vec{R}_j}{2}) \prod_{l'=4}^6 \phi(\vec{r}_{l'} + \frac{\vec{R}_j}{2})] d^3 r_1 \dots d^3 r_6, \quad (3.18)$$

and

$$N_{ij} = \int \prod_{k=1}^3 \phi^+(\vec{r}_k - \frac{\vec{R}_i}{2}) \prod_{k'=4}^6 \phi^+(\vec{r}_{k'} + \frac{\vec{R}_i}{2}) \mathcal{A} [\prod_{l=1}^3 \phi(\vec{r}_l - \frac{\vec{R}_j}{2}) \prod_{l'=4}^6 \phi(\vec{r}_{l'} + \frac{\vec{R}_j}{2})] d^3 r_1 \dots d^3 r_6, \quad (3.19)$$

with $\phi(\vec{r}) = g(\vec{r}, b)$ given by (3.14). These forms are much easier to handle in actual calculations. They allow to reduce the $6q$ matrix elements to two-body matrix elements.

Moreover the distances R_i play now the role of a generator coordinate [4] and lead to a better understanding of the relation between the resonating group method and the generator coordinate method [28].

B. Scattering states

For scattering states the expansion (3.12) holds up to a finite distance $R = R_c$, depending on the range of the interaction. Beyond R_c , $\chi(\vec{R})$ becomes the usual combination of Hankel functions containing the S -matrix. Because practical calculations of both bound state and scattering states are done in terms of partial waves, we first give the partial wave expansion of Eq. (3.12) in terms of locally peaked wave functions with a definite angular momentum l and projection m :

$$\chi_{lm}(\vec{R}) = \sum_{i=1}^N C_i^{(l)} \chi_i^{(l)}(R) Y_{lm}(\hat{R}) , \quad (3.20)$$

with the explicit form of $\chi_i^{(l)}$ given by

$$\chi_i^{(l)}(R) = 4\pi \left(\frac{3}{2\pi b^2}\right)^{3/4} e^{-\frac{3}{4b^2}(R^2 + R_i^2)} i_l\left(\frac{3}{2b^2}RR_i\right) , \quad (3.21)$$

where i_l is the modified spherical Bessel function [29]. When we treat the scattering problem, the form (3.21) holds up to $R \leq R_c$ only. In fact in this case the relative wave function is expanded in terms of $\tilde{\chi}^{(l)}$ as

$$\chi^{(l)}(R) = \sum_{i=1}^N C_i^{(l)} \tilde{\chi}_i^{(l)}(R) , \quad (3.22)$$

where

$$\begin{aligned} \tilde{\chi}_i^{(l)}(R) &= \alpha_i^{(l)} \chi_i^{(l)}(R) , & (R \leq R_c) \\ \tilde{\chi}_i^{(l)}(R) &= h_l^{(-)}(kR) + S_i^{(l)} h_l^{(+)}(kR) , & (R \geq R_c) \end{aligned} \quad (3.23)$$

with $\chi_i^{(l)}(R)$ defined by Eq. (3.21). Here k is the wave number $k = \sqrt{2\mu E_{rel}}$ and $h_l^{(-)}$ and $h_l^{(+)}$ are spherical Hankel functions [29]. The coefficients $\alpha_i^{(l)}$ and $S_i^{(l)}$ are determined

from the continuity of $\tilde{\chi}_i^{(l)}$ and its derivative at $R = R_c$. The coefficients $C_i^{(l)}$ of (3.20) are normalized such that $\sum_{i=1}^N C_i^{(l)} = 1$. Then the S -matrix is given in terms of the coefficients $C_i^{(l)}$ as

$$S^{(l)} = \sum_{i=1}^N C_i^{(l)} S_i^{(l)} . \quad (3.24)$$

The method of determining the expansion coefficients is described in detail by Oka and Yazaki [27].

C. Coupled channels

Here we consider more than one channel. In this case, based on Eq. (3.1), the RGM equation becomes a system of coupled channel equations for χ_β

$$\sum_\beta \int \mathcal{L}_{\alpha\beta}(\vec{R}', \vec{R}) \chi_\beta(\vec{R}) d^3R = \sum_\beta \int [\mathcal{H}_{\alpha\beta}(\vec{R}', \vec{R}) - E \mathcal{N}_{\alpha\beta}(\vec{R}', \vec{R})] \chi_\beta(\vec{R}) d^3R = 0 . \quad (3.25)$$

Usually the normalisation kernel $\mathcal{N}_{\alpha\beta}$ is not diagonal because of the antisymmetrisation. For a given SI sector one can establish which are the $6q$ states of (3.2) allowed by the Pauli principle [30]. Here we consider the $l = 0$ partial waves i. e. we study the 3S_1 and 1S_0 phase shifts. In this case, according to [30], the $6q$ allowed states are $NN, \Delta\Delta$ and CC . The NN and $\Delta\Delta$ states are easy to define directly from Eq. (3.1). For CC states we adopt the definition of Ref. [31] which is more appropriate for RGM calculation. This CC state of six quarks allows some ‘‘color polarisation’’ of the $6q$ system in the interaction region. It is defined in the following way

$$|CC\rangle = \alpha|NN\rangle + \beta|\Delta\Delta\rangle + \gamma\mathcal{A}_{STC}|\Delta\Delta\rangle , \quad (3.26)$$

with

$$\mathcal{A}_{STC} = \frac{1}{10} [1 - \sum_{i=1}^3 \sum_{j=4}^6 P_{ij}^\sigma P_{ij}^f P_{ij}^c] , \quad (3.27)$$

where P_{ij}^σ, P_{ij}^f and P_{ij}^c are the exchange operators in the spin, isospin and color space respectively defined by (3.5). From the orthonormality conditions $\langle CC|CC\rangle = 1$, $\langle CC|NN\rangle = 0$ and $\langle CC|\Delta\Delta\rangle = 0$ one can determine the coefficients α , β and γ so that

$$|CC\rangle = -\frac{\sqrt{5}}{6}|NN\rangle + \frac{1}{3}|\Delta\Delta\rangle - \frac{15}{4}\mathcal{A}_{STC}|\Delta\Delta\rangle. \quad (3.28)$$

The important feature in the definition of the CC -state is that the eigenvalue of the color $SU(3)$ Casimir operator is 12 for each $3q$ cluster. This tells us that C is a color octet state and thus explains why we call the CC -state a hidden color state. Note that at zero separation between quarks (shell model basis) the CC state above is the same as that introduced by Harvey. The two differ only at finite separation distances. To see the identity with Harvey's CC state [30] at zero separation one can combine it with the NN and $\Delta\Delta$ states as defined by Eq. (3.1) to get symmetry states of the form $|[f]_{FS}[222]_C; \tilde{g}_{FSC}\rangle$ where \tilde{g} is the representation resulting from the inner product of $[f]_{FS}$ and $[222]_C$ which is conjugate with the symmetry g of an orbital state such as to produce a totally antisymmetric $6q$ state. Comparing Table 3 of Ref. [31] with that of Harvey's [30] Table 1 one can see that the coefficients of this basis transformation are identical which proves the identity of the hidden color state (3.28) with that of Harvey at $R = 0$. Note that Harvey's definition [30] of CC is more appropriate for generator coordinate method than for RGM calculations.

IV. SIX-BODY MATRIX ELEMENTS

The method to compute the six-body matrix elements is explained in some detail in the appendix. In Tables I & II we give the results for diagonal and off-diagonal matrix elements of the channels NN , $\Delta\Delta$ and CC to be used in coupled channel calculations of the 3S_1 and 1S_0 phase shifts respectively. Although we apply the $SU(3)$ version of the GBE model the matrix elements of $\sigma_i \cdot \sigma_j \tau_i \cdot \tau_j$ and $\sigma_i \cdot \sigma_j \tau_i \cdot \tau_j P_{36}^{f\sigma c}$ needed in $SU(2)$ calculations are also indicated. In fact they are used in calculating the expectation value of $\sigma_i \cdot \sigma_j \lambda_i^8 \cdot \lambda_j^8$ by subtracting them from $\sigma_i \cdot \sigma_j \lambda_i^f \cdot \lambda_j^f$ because there is no K meson exchange. Moreover the values we found can be considered as a validity test of our method because they are in full agreement with Table 1 of Ref. [32].

V. NUMERICAL RESULTS

We perform RGM calculation as described above for NN , $NN + \Delta\Delta$ and $NN + \Delta\Delta + CC$ channels. In all cases the size parameter of the Gaussian (3.14) is fixed at $b = 0.44$ fm by the stability condition (see for example Ref. [1])

$$\frac{\partial}{\partial b} \langle \phi | H | \phi \rangle = 0 , \quad (5.1)$$

where ϕ is a variational solution of the Hamiltonian (2.1) for a ground state $3q$ system. This solution is fully symmetric in the orbital space and is chosen to be of the form

$$\phi = \prod_{i=1}^3 g(\vec{r}_i, b) , \quad (5.2)$$

with $g(\vec{r}_i, b)$ of (3.14).

Either if we take one, two or three channels namely NN , $NN + \Delta\Delta$ or $NN + \Delta\Delta + CC$ we found that a number of 15 Gaussians in the expansion (3.12) is large enough to obtain convergence. In all cases the result is stable at the matching radius $R_c = 4.5$ fm. In Figs. 1 & 2 we show the phase shifts as a function of the relative momentum k obtained from one, two and three coupled channels. One can see that the addition to NN of the $\Delta\Delta$ channel alone or of both $\Delta\Delta$ and CC channels brings a very small change in the 3S_1 and 1S_0 phase shifts below 2.5 fm $^{-1}$, making the repulsion slightly weaker. The CC channel brings slightly more repulsion than the $\Delta\Delta$ channel. In fact the role of CC channels is expected to increase for larger values of k , or alternatively smaller separation distances between nucleons, where they could bring an important contribution. Of course, the contribution of the CC channels to the NN phase shifts vanishes at larger separations because of their color structure. The conclusion regarding the minor contribution of $\Delta\Delta$ and CC channels to the phase shifts below 2.5 fm $^{-1}$ is similar for results based on the OGE model (see for example [31]). Thus for $l = 0$ waves it is good enough to perform one channel calculations in the lab energy interval 0-350 MeV.

We recall that the pseudoscalar exchange interaction (2.4) contains both a short range part, responsible for the repulsion, and a long range Yukawa-type potential which brings

attraction in the NN potential. In order to see the difference in the amount of repulsion induced by the GBE and that induced by the OGE interaction we repeated the one channel (NN) calculations above by removing the Yukawa-type part. We compared the resulting phase shifts with those of Fig. 2 of Ref. [31] obtained with an OGE interaction parametrized such as to satisfy the stability condition (5.1). We found that in the GBE model the repulsion is much stronger and corresponds to a hard core radius $r_0^{GBE} = 0.68$ fm (versus $r_0^{OGE} = 0.30$ fm) in the 3S_1 and $r_0^{GBE} = 0.81$ fm (versus $r_0^{OGE} = 0.35$ fm) in the 1S_0 partial waves. The radius r_0 was extracted from the phase shifts at small k , which is approximately given by $\delta = -kr_0$. One can also see that the repulsion induced by the GBE interaction in the 3S_1 partial wave is weaker than that induced in the 1S_0 partial wave. This is consistent with our previous result [22] where we found that the height of the repulsive core is lower for 3S_1 than for 1S_0 , as mentioned in the introduction. Thus the OGE model gives less repulsion than the GBE model. In Ref. [33] the stronger repulsion induced by the GBE interaction is viewed as a welcome feature in correctly describing the phase shifts above $E_{lab} = 350$ MeV.

A note of caution is required regarding the removal of the long-range Yukawa part of the interaction (2.4) with the parametrization (2.5) which contains a rather large coupling constant $g_{\eta'q}^2/(4\pi) = 2.7652$. The η' -meson exchange is responsible for describing correctly the $\Delta - N$ splitting. If the long-range Yukawa part is removed, the model fails to describe this splitting because the contribution coming from the second term of (2.4) for $\gamma = \eta'$ becomes too large in a $3q$ system in the parametrization (2.5). We recall that the contribution to N of the short-range η' -meson exchange part is proportional to a factor of 2 and the contribution to Δ to a factor -2 [9], which brings Δ too low and N too high if the Yukawa part is removed. In these circumstances two or three coupled channel calculations become meaningless.

It is also interesting to see the behaviour of the relative wave function $\chi^{l=0}$ of Eq. (3.22) at short distances. Instead of $\chi^{l=0}$ it is more appropriate [27] to introduce a renormalized wave function as

$$\tilde{\chi}_{\alpha}^{l=0}(R) = \sum_{\beta} \int dR' [N_{\beta\alpha}^{l=0}(R, R')]^{1/2} \chi_{\beta}^{l=0}(R') , \quad (5.3)$$

where the quantity to be integrated contains the $l = 0$ component of the norm N . In Fig. 3 we show results for the above function for the 3S_1 wave at $k = 1 \text{ fm}^{-1}$ both for the one and the three channel cases. One can see that for $R < 1 \text{ fm}$ the two functions are entirely different, in the three channel case a node being present. If the renormalization was made with the norm N instead of its square, as in Eq. (5.3), no node would have been present. The existence of a node is related to the presence of the $[42]_O$ configuration in the wave function (see e.g. [20]). Here, whenever it appears, it is due to the cancellation of the positive and negative components of the wave function, but the lack of a node does not exclude a repulsive potential. In a renormalized wave function the amplitudes of positive and negative components change their values depending on the multiplicative factor N or $N^{1/2}$ so the node could appear in one renormalization definition but not in the other. On the other hand, as discussed above, the phase shift changes insignificantly when one goes from one channel to three channels, and this can also be seen in the asymptotic form of the wave function beyond $R = 1 \text{ fm}$, although in the overlap region the two functions are entirely different. The above behaviour of the wave function is very similar to that found in Ref. [33] where no long-range part is present in the schematic quark-quark potential due to pion exchange.

In Fig. 4 we represent the 3S_1 and 1S_0 phase shifts of Figs. 1 & 2 in the one channel case (NN) again with the Yukawa part included, but this time as a function of $E_{lab} = 2\hbar^2 k^2 / 3m$ with $m = m_{u,d}$ of (2.5). This is to show that in the GBE model the two phase shifts are very near each other, with $\delta(^3S_1)$ slightly lower than $\delta(^1S_0)$. Contrary, in OGE calculations as example those of Fig. 2 of Ref. [31] one obtaines $\delta(^3S_1) > \delta(^1S_0)$. In calculations based on the OGE model the difference between the two phase shifts is reduced by the addition of a scalar potential acting at a nucleon level with a larger attractive strength in the 1S_0 channel than in the 3S_1 channel [5].

A major difference between the GBE $\delta(^3S_1)$ and $\delta(^1S_0)$ is expected to appear after the inclusion of a quark-quark tensor force [34]. This will modify only the 3S_1 phase shift.

VI. CONCLUSIONS

This work is a further important step in our previous studies [21,22] of the NN problem. We consider the two interacting nucleons as a $6q$ system described by a Hamiltonian containing a linear confinement plus a pseudoscalar (meson) exchange interaction between quarks.

Previously we derived an NN potential in an adiabatic approximation. The present study is based on a dynamical approach of the NN interaction, namely the resonating group method. We perform one, two and three coupled channel calculations for the 3S_1 and 1S_0 phase shifts for laboratory energies up to about 350 MeV.

Our conclusions are :

1. The phase shifts present a behaviour typical for strongly repulsive potentials. We find that this repulsion, which is induced by pseudoscalar meson exchange is stronger than that produced by the OGE interaction.
2. In the 1S_0 partial wave the repulsion is stronger than in 3S_1 partial wave as our previous studies suggested.
3. Our results prove that in the laboratory energy interval 0-350 MeV the one channel approximation is entirely satisfactory.

Finally in future calculation, in order to describe the 3S_1 phase shift the tensor force is compulsory and this is our following major step.

Acknowledgements. We are most grateful to Kiyotaka Shimizu for help in understanding the resonating group method techniques and for constructive criticism in preparing the manuscript.

Appendix A

The method to compute the six-body matrix elements is explained here using the example of $S = 1, I = 0$ case.

We know that for the nucleon, the spin-flavor wavefunction is given by

$$\psi_N = \frac{1}{\sqrt{2}} [\chi^\rho \phi^\rho + \chi^\lambda \phi^\lambda] , \quad (0.1)$$

where χ and ϕ are the spin and flavor parts respectively. For the spin parts we have

$$\begin{aligned} \chi_{1/2}^\rho &= \frac{1}{\sqrt{2}} (\uparrow\downarrow\uparrow - \downarrow\uparrow\uparrow) , \\ \chi_{-1/2}^\rho &= \frac{1}{\sqrt{2}} (\uparrow\downarrow\downarrow - \downarrow\uparrow\downarrow) , \\ \chi_{1/2}^\lambda &= \frac{1}{\sqrt{6}} (\uparrow\downarrow\uparrow + \downarrow\uparrow\uparrow - 2\uparrow\uparrow\downarrow) , \\ \chi_{-1/2}^\lambda &= \frac{-1}{\sqrt{6}} (\uparrow\downarrow\downarrow + \downarrow\uparrow\downarrow - 2\downarrow\downarrow\uparrow) , \end{aligned} \quad (0.2)$$

and similarly for the flavor parts with \uparrow replaced by u and \downarrow replaced by d . Then for $\beta = NN$, the Eq. (3.2) becomes

$$\Phi_{NN}^{SI} = \frac{1}{2} \sum C_{s_1 s_2 s}^{\frac{1}{2} \frac{1}{2} S} C_{\tau_1 \tau_2 \tau}^{\frac{1}{2} \frac{1}{2} I} [\chi_{s_1}^\rho(1) \phi_{\tau_1}^\rho(1) + \chi_{s_1}^\lambda(1) \phi_{\tau_1}^\lambda(1)] [\chi_{s_2}^\rho(2) \phi_{\tau_2}^\rho(2) + \chi_{s_2}^\lambda(2) \phi_{\tau_2}^\lambda(2)] , \quad (0.3)$$

where S and I are the spin and isospin of the NN system. $\chi(i)$ and $\phi(i)$ are the spin and flavor parts of the i^{th} nucleon. For $S = S_z = 1$ and $I = I_z = 0$, after inserting the values of the corresponding Clebsch-Gordan coefficients we have

$$\begin{aligned} \Phi_{NN}^{10} &= \frac{1}{2\sqrt{2}} \{ [\chi_{1/2}^\rho(1) \phi_{1/2}^\rho(1) + \chi_{1/2}^\lambda(1) \phi_{1/2}^\lambda(1)] [\chi_{1/2}^\rho(2) \phi_{-1/2}^\rho(2) + \chi_{1/2}^\lambda(2) \phi_{-1/2}^\lambda(2)] \\ &\quad - [\chi_{1/2}^\rho(1) \phi_{-1/2}^\rho(1) + \chi_{1/2}^\lambda(1) \phi_{-1/2}^\lambda(1)] [\chi_{1/2}^\rho(2) \phi_{1/2}^\rho(2) + \chi_{1/2}^\lambda(2) \phi_{1/2}^\lambda(2)] \} . \end{aligned} \quad (0.4)$$

At this stage we use MATHEMATICA [35]. We introduce Eqs. (0.2) and the equivalent for the flavor parts in (0.4). We get a huge expression with 338 terms depending now on the quantum numbers of the quarks. In the matrix element of an operator O we then get $338^2 = 114244$ terms of the form

$$\langle s_1 s_2 s_3 s_4 s_5 s_6 \tau_1 \tau_2 \tau_3 \tau_4 \tau_5 \tau_6 | O | s'_1 s'_2 s'_3 s'_4 s'_5 s'_6 \tau'_1 \tau'_2 \tau'_3 \tau'_4 \tau'_5 \tau'_6 \rangle , \quad (0.5)$$

where s_i and τ_i ($i = 1, \dots, 6$) stand for the spin and isospin projection of the i^{th} quark. Note that the normal order of particles is implied. Now let us choose $O = \vec{\sigma}_1 \cdot \vec{\sigma}_3 \vec{\lambda}_1^f \cdot \vec{\lambda}_3^f P_{36}^{\sigma f}$, which contains the permutation P_{36} . Then we have

$$\begin{aligned}
& \langle s_1 s_2 s_3 s_4 s_5 s_6 \tau_1 \tau_2 \tau_3 \tau_4 \tau_5 \tau_6 | \vec{\sigma}_1 \cdot \vec{\sigma}_3 \vec{\lambda}_1^f \cdot \vec{\lambda}_3^f P_{36}^{\sigma f} | s'_1 s'_2 s'_3 s'_4 s'_5 s'_6 \tau'_1 \tau'_2 \tau'_3 \tau'_4 \tau'_5 \tau'_6 \rangle \\
&= \langle s_1 s_2 s_3 s_4 s_5 s_6 \tau_1 \tau_2 \tau_3 \tau_4 \tau_5 \tau_6 | \vec{\sigma}_1 \cdot \vec{\sigma}_3 \vec{\lambda}_1^f \cdot \vec{\lambda}_3^f | s'_1 s'_2 s'_6 s'_4 s'_5 s'_3 \tau'_1 \tau'_2 \tau'_6 \tau'_4 \tau'_5 \tau'_3 \rangle \\
&= \langle s_1 s_3 \tau_1 \tau_3 | \vec{\sigma}_1 \cdot \vec{\sigma}_3 \vec{\lambda}_1^f \cdot \vec{\lambda}_3^f | s'_1 s'_6 \tau'_1 \tau'_6 \rangle \delta_{s_2}^{s'_2} \delta_{s_4}^{s'_4} \delta_{s_5}^{s'_5} \delta_{s_6}^{s'_6} \delta_{\tau_2}^{\tau'_2} \delta_{\tau_4}^{\tau'_4} \delta_{\tau_5}^{\tau'_5} \delta_{\tau_6}^{\tau'_6} \\
&= \langle s_1 s_3 | \vec{\sigma}_1 \cdot \vec{\sigma}_3 | s'_1 s'_6 \rangle \langle \tau_1 \tau_3 | \vec{\lambda}_1^f \cdot \vec{\lambda}_3^f | \tau'_1 \tau'_6 \rangle \delta_{s_2}^{s'_2} \delta_{s_4}^{s'_4} \delta_{s_5}^{s'_5} \delta_{s_6}^{s'_6} \delta_{\tau_2}^{\tau'_2} \delta_{\tau_4}^{\tau'_4} \delta_{\tau_5}^{\tau'_5} \delta_{\tau_6}^{\tau'_6} . \tag{0.6}
\end{aligned}$$

This shows how a six-body matrix element can be reduced to the calculation of two-body matrix elements. The necessary nonzero two-body matrix elements are

$$\begin{aligned}
& \langle \uparrow\uparrow | \vec{\sigma}_1 \cdot \vec{\sigma}_2 | \uparrow\uparrow \rangle = \langle \downarrow\downarrow | \vec{\sigma}_1 \cdot \vec{\sigma}_2 | \downarrow\downarrow \rangle = 1 , \\
& \langle \uparrow\downarrow | \vec{\sigma}_1 \cdot \vec{\sigma}_2 | \uparrow\downarrow \rangle = \langle \downarrow\uparrow | \vec{\sigma}_1 \cdot \vec{\sigma}_2 | \downarrow\uparrow \rangle = -1 , \\
& \langle \uparrow\downarrow | \vec{\sigma}_1 \cdot \vec{\sigma}_2 | \downarrow\uparrow \rangle = \langle \downarrow\uparrow | \vec{\sigma}_1 \cdot \vec{\sigma}_2 | \uparrow\downarrow \rangle = 2 , \\
& \langle uu | \vec{\lambda}_1^f \cdot \vec{\lambda}_2^f | uu \rangle = \langle dd | \vec{\lambda}_1^f \cdot \vec{\lambda}_2^f | dd \rangle = 4/3 , \\
& \langle ud | \vec{\lambda}_1^f \cdot \vec{\lambda}_2^f | ud \rangle = \langle du | \vec{\lambda}_1^f \cdot \vec{\lambda}_2^f | du \rangle = -2/3 , \\
& \langle ud | \vec{\lambda}_1^f \cdot \vec{\lambda}_2^f | du \rangle = \langle du | \vec{\lambda}_1^f \cdot \vec{\lambda}_2^f | ud \rangle = 2 . \tag{0.7}
\end{aligned}$$

MATHEMATICA is then used to compute systematically the sum of the 114244 terms stemming from Eq. (0.4).

In Tables I & II all required six-body matrix elements obtained by this technique are listed.

REFERENCES

- [1] M. Oka and K. Yazaki, “Quarks and Nuclei”, International Review of Nuclear Physics, vol. 1, ed. W. Weise (World Scientific, Singapore, 1985), p. 489
- [2] F. Myhrer and J. Wroldsen, Rev. Mod. Phys. **60** (1988) 629
- [3] K. Shimizu, Rep. Prog. Phys. **52** (1989) 1 and references therein
- [4] K. Shimizu, S. Tacheuchi and A. J. Buchmann, Progr. Theor. Phys. Suppl. **137** (2000) 43
- [5] M. Oka and K. Yazaki, Nucl. Phys. **A402** (1983) 447
- [6] A. M. Kusainov, V. G. Neudatchin and I. T. Obukhovsky, Phys. Rev. **C44** (1991) 2343
- [7] Z. Zhang, A. Faessler, U. Straub and L. Ya. Glozman, Nucl. Phys. **A578** (1994) 573; A. Valcarce, A. Buchmann, F. Fernández and A. Faessler, Phys. Rev. **C50** (1994) 2246
- [8] Y. Fujiwara, C. Nakamoto and Y. Suzuki, Phys. Rev. Lett. **76** (1996) 2242
- [9] L. Ya. Glozman and D. O. Riska, Phys. Rep. **268** (1996) 263
- [10] L. Ya. Glozman, Z. Papp and W. Plessas, Phys. Lett. **B381** (1996) 311
- [11] L. Ya. Glozman, Z. Papp, W. Plessas, K. Varga and R. F. Wagenbrunn, Nucl. Phys. **A623** (1997) 90c
- [12] L. Ya. Glozman, W. Plessas, K. Varga and R. F. Wagenbrunn, Phys. Rev. **D58** (1998) 094030
- [13] L. Ya. Glozman, Nucl. Phys. **A663&664** (2000) 103c
- [14] A. Manohar and H. Georgi, Nucl. Phys. **B234** (1994) 189
- [15] It was noticed first by D. Robson, see *Proc. Topical Conf. on Nuclear Chromodynamics*, World Scientific (Singapore 1988) that a flavor-spin interaction of type $-\sum_{i < j} \lambda_i^F \cdot \lambda_j^F \vec{\sigma}_i \cdot \vec{\sigma}_j$ gives the position of the Roper resonance below the first excited negative parity states,

in agreement with the experiment. However Robson's conclusion that any contact interaction, irrespective of its flavor-spin or color-spin structure, would give the desired order, was incorrect

- [16] D. O. Riska and G. E. Brown, Nucl. Phys. **A653** (1999) 251
- [17] H. Collins and H. Georgi, Phys. Rev. **D59** (1999) 094010
- [18] C. D. Carone, Nucl. Phys. **A663&664** (2000) 687c
- [19] S. Sasaki, hep-ph/0004252
- [20] Fl. Stancu, S. Pepin and L. Ya. Glozman, Phys. Rev. **C56** (1997) 2779
- [21] D. Bartz and Fl. Stancu, Phys. Rev. **C59** (1999) 1756
- [22] D. Bartz and Fl. Stancu, Phys. Rev. **C60** (1999) 055207
- [23] J. A. Wheeler, Phys. Rev. **52** (1937), 1107
- [24] K. Wildermuth and Y. C. Tang, *A Unified Theory of the Nucleus* (Vieweg Braunschweig, 1977)
- [25] M. Kamimura, Prog. Theor. Phys. Suppl. **62** (1977) 236
- [26] Fl. Stancu and L. Ya. Glozman, nucl-th/9906058
- [27] M. Oka and K. Yazaki, Phys. Lett. **90B** (1980) 41, M. Oka and K. Yazaki, Progr. Theor. Phys. **66** (1981) 556, 572
- [28] M. Cvjetić, B. Golli, N. Mankoč-Borštnik and M. Rosina, Nucl. Phys. **A395** (1983) 349
- [29] M. Abramowitz and I. A. Stegun, *Handbook of Mathematical Functions* (Dover edition, 1964)
- [30] M. Harvey, Nucl. Phys. **A352** (1981) 301 and 326; **A481** (1988) 834
- [31] A. Faessler, F. Fernández, G. Lübeck and K. Shimizu, Nucl. Phys. **A402** (1983) 555

- [32] K. Shimizu, Phys. Let. **148B** (1984) 418
- [33] K. Shimizu and L. Ya. Glozman, Phys. Lett. **B477** (2000) 59
- [34] W. Plessas, L. Ya. Glozman, K. Varga and R. F. Wagenbrunn, Proc. 2nd International Conference on *Perspectives in Hadronic Physics*, Trieste, 1999, eds. S. Boffi et al., (World Scientific, Singapore, 2000), p. 136; see also R. F. Wagenbrunn, L. Ya. Glozman, W. Plessas, K. Varga, Nucl. Phys. **A663&664** (2000) 703c
- [35] S. Wolfram, The Mathematica book, Wolfram Media/Cambridge University Press, Cambridge, 1996

TABLES

 TABLE I. Matrix elements $\langle \alpha | O | \beta \rangle$ of different operators O for (S,I) = (1,0).

α	NN	NN	$\Delta\Delta$	NN	$\Delta\Delta$	CC
β	NN	$\Delta\Delta$	$\Delta\Delta$	CC	CC	CC
1	972	0	972	0	0	972
$P_{36}^{f\sigma c}$	-12	48	12	-144	288	-756
$\lambda_1^c \cdot \lambda_2^c$	-2592	0	-2592	0	0	-648
$\lambda_3^c \cdot \lambda_6^c$	0	0	0	0	0	-1296
$\lambda_1^c \cdot \lambda_2^c P_{36}^{f\sigma c}$	32	-128	-32	384	-768	72
$\lambda_3^c \cdot \lambda_6^c P_{36}^{f\sigma c}$	-64	256	64	96	-192	1152
$\lambda_1^c \cdot \lambda_3^c P_{36}^{f\sigma c}$	32	-128	-32	384	-768	720
$\lambda_1^c \cdot \lambda_6^c P_{36}^{f\sigma c}$	32	-128	-32	-48	96	720
$\lambda_1^c \cdot \lambda_4^c P_{36}^{f\sigma c}$	-16	64	16	24	-48	1260
$\sigma_1 \cdot \sigma_2 \tau_1 \cdot \tau_2$	4860	0	972	0	0	108
$\sigma_3 \cdot \sigma_6 \tau_3 \cdot \tau_6$	-900	576	1980	0	0	1116
$\sigma_1 \cdot \sigma_2 \tau_1 \cdot \tau_2 P_{36}^{f\sigma c}$	-444	48	12	-720	288	588
$\sigma_3 \cdot \sigma_6 \tau_3 \cdot \tau_6 P_{36}^{f\sigma c}$	708	48	1596	240	672	-1092
$\sigma_1 \cdot \sigma_3 \tau_1 \cdot \tau_3 P_{36}^{f\sigma c}$	132	336	12	-720	288	-420
$\sigma_1 \cdot \sigma_6 \tau_1 \cdot \tau_6 P_{36}^{f\sigma c}$	132	48	12	336	-96	-420
$\sigma_1 \cdot \sigma_4 \tau_1 \cdot \tau_4 P_{36}^{f\sigma c}$	36	-144	-36	228	288	-1260
$\sigma_1 \cdot \sigma_2 \lambda_1^f \cdot \lambda_2^f$	4536	0	1296	0	0	-18
$\sigma_3 \cdot \sigma_6 \lambda_3^f \cdot \lambda_6^f$	-864	576	1584	0	0	1020
$\sigma_1 \cdot \sigma_2 \lambda_1^f \cdot \lambda_2^f P_{36}^{f\sigma c}$	-376	64	16	-672	384	706
$\sigma_3 \cdot \sigma_6 \lambda_3^f \cdot \lambda_6^f P_{36}^{f\sigma c}$	784	32	1520	216	528	-1024
$\sigma_1 \cdot \sigma_3 \lambda_1^f \cdot \lambda_3^f P_{36}^{f\sigma c}$	104	304	16	-672	384	-332
$\sigma_1 \cdot \sigma_6 \lambda_1^f \cdot \lambda_6^f P_{36}^{f\sigma c}$	104	64	16	340	-200	-332
$\sigma_1 \cdot \sigma_4 \lambda_1^f \cdot \lambda_4^f P_{36}^{f\sigma c}$	44	-152	-32	278	164	-1197
$\sigma_1 \cdot \sigma_2 \lambda_1^{f,0} \cdot \lambda_2^{f,0}$	-648	0	648	0	0	-252
$\sigma_3 \cdot \sigma_6 \lambda_3^{f,0} \cdot \lambda_6^{f,0}$	72	0	-792	0	0	-192
$\sigma_1 \cdot \sigma_2 \lambda_1^{f,0} \cdot \lambda_2^{f,0} P_{36}^{f\sigma c}$	136	32	8	96	192	236
$\sigma_3 \cdot \sigma_6 \lambda_3^{f,0} \cdot \lambda_6^{f,0} P_{36}^{f\sigma c}$	152	-32	-152	-48	-288	136
$\sigma_1 \cdot \sigma_3 \lambda_1^{f,0} \cdot \lambda_3^{f,0} P_{36}^{f\sigma c}$	-56	-64	8	96	192	176
$\sigma_1 \cdot \sigma_6 \lambda_1^{f,0} \cdot \lambda_6^{f,0} P_{36}^{f\sigma c}$	-56	32	8	8	-208	176
$\sigma_1 \cdot \sigma_4 \lambda_1^{f,0} \cdot \lambda_4^{f,0} P_{36}^{f\sigma c}$	16	-16	8	-20	-248	126
factor	1 972	$\sqrt{5}$ 972	1 972	$\sqrt{5}$ 972	1 972	1 972

TABLE II. Matrix elements $\langle \alpha|O|\beta \rangle$ of different operators O for (S,I) = (0,1).

α	NN	NN	$\Delta\Delta$	NN	$\Delta\Delta$	CC
β	NN	$\Delta\Delta$	$\Delta\Delta$	CC	CC	CC
1	972	0	972	0	0	972
$P_{36}^{f\sigma c}$	-12	48	12	-144	288	-756
$\lambda_1^c \cdot \lambda_2^c$	-2592	0	-2592	0	0	-648
$\lambda_3^c \cdot \lambda_6^c$	0	0	0	0	0	-1296
$\lambda_1^c \cdot \lambda_2^c P_{36}^{f\sigma c}$	32	-128	-32	384	-768	72
$\lambda_3^c \cdot \lambda_6^c P_{36}^{f\sigma c}$	-64	256	64	96	-192	1152
$\lambda_1^c \cdot \lambda_3^c P_{36}^{f\sigma c}$	32	-128	-32	384	-768	720
$\lambda_1^c \cdot \lambda_6^c P_{36}^{f\sigma c}$	32	-128	-32	-48	96	720
$\lambda_1^c \cdot \lambda_4^c P_{36}^{f\sigma c}$	-16	64	16	24	-48	1260
$\sigma_1 \cdot \sigma_2 \tau_1 \cdot \tau_2$	4860	0	972	0	0	108
$\sigma_3 \cdot \sigma_6 \tau_3 \cdot \tau_6$	-900	576	1980	0	0	1116
$\sigma_1 \cdot \sigma_2 \tau_1 \cdot \tau_2 P_{36}^{f\sigma c}$	-444	48	12	-720	288	588
$\sigma_3 \cdot \sigma_6 \tau_3 \cdot \tau_6 P_{36}^{f\sigma c}$	708	48	1596	240	672	-1092
$\sigma_1 \cdot \sigma_3 \tau_1 \cdot \tau_3 P_{36}^{f\sigma c}$	132	336	12	-720	288	-420
$\sigma_1 \cdot \sigma_6 \tau_1 \cdot \tau_6 P_{36}^{f\sigma c}$	132	48	12	336	-96	-420
$\sigma_1 \cdot \sigma_4 \tau_1 \cdot \tau_4 P_{36}^{f\sigma c}$	36	-144	-36	228	288	-1260
$\sigma_1 \cdot \sigma_2 \lambda_1^f \cdot \lambda_2^f$	4536	0	1296	0	0	-126
$\sigma_3 \cdot \sigma_6 \lambda_3^f \cdot \lambda_6^f$	-1008	576	1440	0	0	948
$\sigma_1 \cdot \sigma_2 \lambda_1^f \cdot \lambda_2^f P_{36}^{f\sigma c}$	-376	64	16	-672	384	814
$\sigma_3 \cdot \sigma_6 \lambda_3^f \cdot \lambda_6^f P_{36}^{f\sigma c}$	832	32	1568	232	496	-976
$\sigma_1 \cdot \sigma_3 \lambda_1^f \cdot \lambda_3^f P_{36}^{f\sigma c}$	104	304	16	-672	384	-260
$\sigma_1 \cdot \sigma_6 \lambda_1^f \cdot \lambda_6^f P_{36}^{f\sigma c}$	104	64	16	364	-248	-260
$\sigma_1 \cdot \sigma_4 \lambda_1^f \cdot \lambda_4^f P_{36}^{f\sigma c}$	36	-168	-48	298	124	-1155
$\sigma_1 \cdot \sigma_2 \lambda_1^{f,0} \cdot \lambda_2^{f,0}$	-648	0	648	0	0	-468
$\sigma_3 \cdot \sigma_6 \lambda_3^{f,0} \cdot \lambda_6^{f,0}$	-216	0	-1080	0	0	-336
$\sigma_1 \cdot \sigma_2 \lambda_1^{f,0} \cdot \lambda_2^{f,0} P_{36}^{f\sigma c}$	136	32	8	96	192	452
$\sigma_3 \cdot \sigma_6 \lambda_3^{f,0} \cdot \lambda_6^{f,0} P_{36}^{f\sigma c}$	248	-32	-56	-16	-352	232
$\sigma_1 \cdot \sigma_3 \lambda_1^{f,0} \cdot \lambda_3^{f,0} P_{36}^{f\sigma c}$	-56	-64	8	96	192	320
$\sigma_1 \cdot \sigma_6 \lambda_1^{f,0} \cdot \lambda_6^{f,0} P_{36}^{f\sigma c}$	-56	32	8	56	-304	320
$\sigma_1 \cdot \sigma_4 \lambda_1^{f,0} \cdot \lambda_4^{f,0} P_{36}^{f\sigma c}$	0	-48	-24	20	-328	210
factor	$\frac{1}{972}$	$\frac{\sqrt{5}}{972}$	$\frac{1}{972}$	$\frac{\sqrt{5}}{972}$	$\frac{1}{972}$	$\frac{1}{972}$

FIGURES

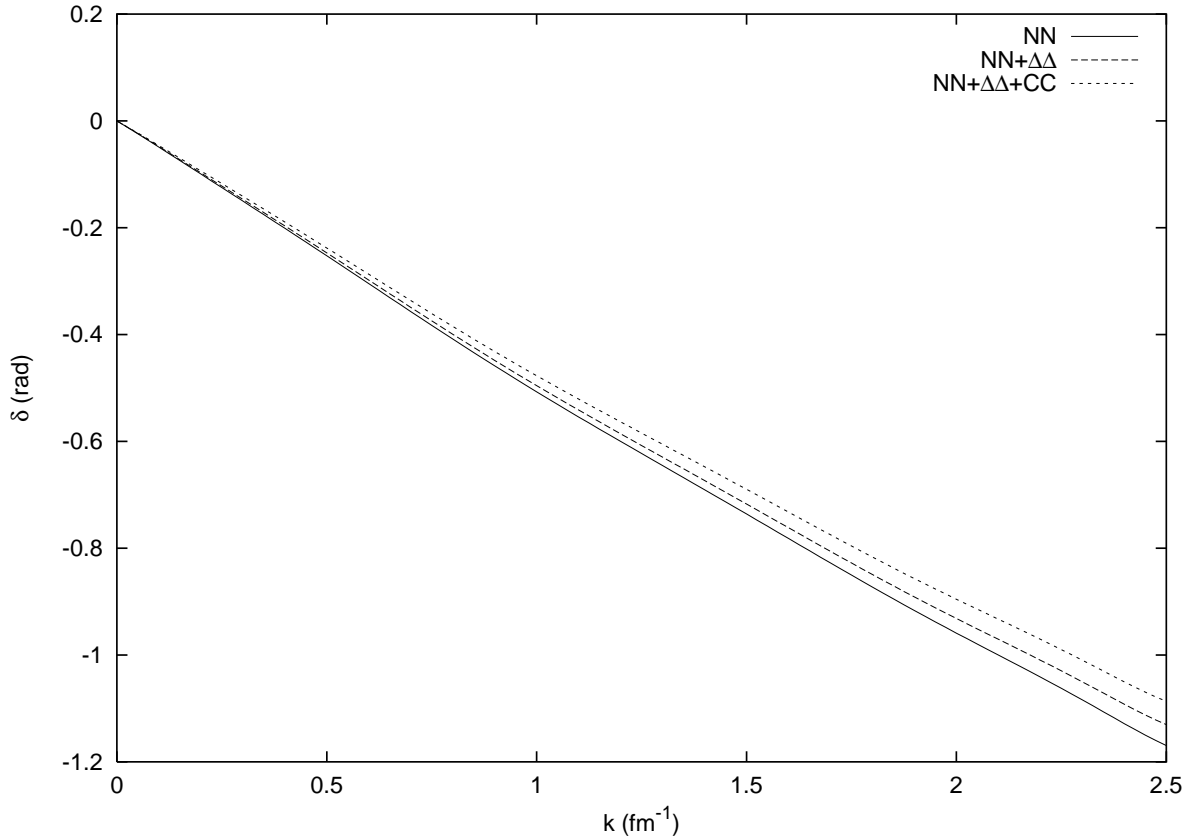


FIG. 1. 3S_1 NN scattering phase shift as a function of k . The solid line shows the result for the NN channel only, the dotted line for the $NN+\Delta\Delta$ and the dashed line for the $NN+\Delta\Delta+CC$ coupled channels.

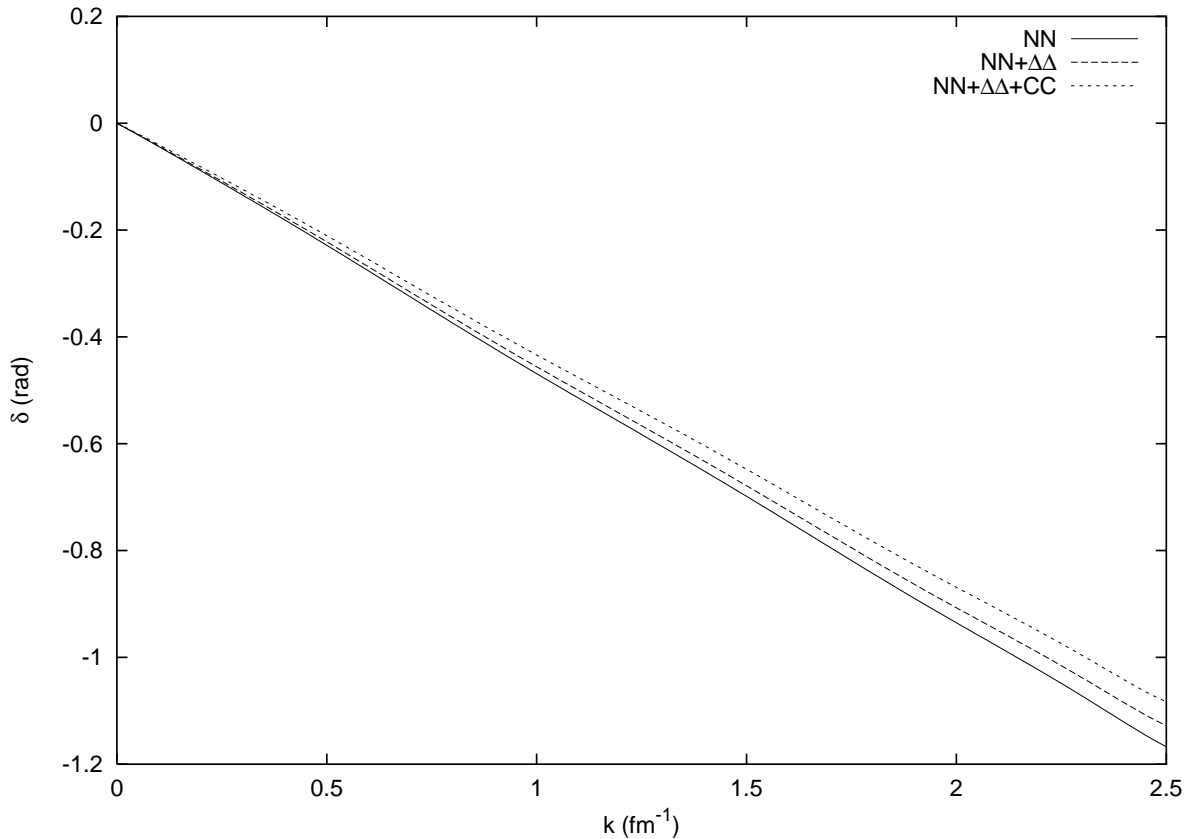


FIG. 2. Same as Fig. 1 but for the 1S_0 partial wave.

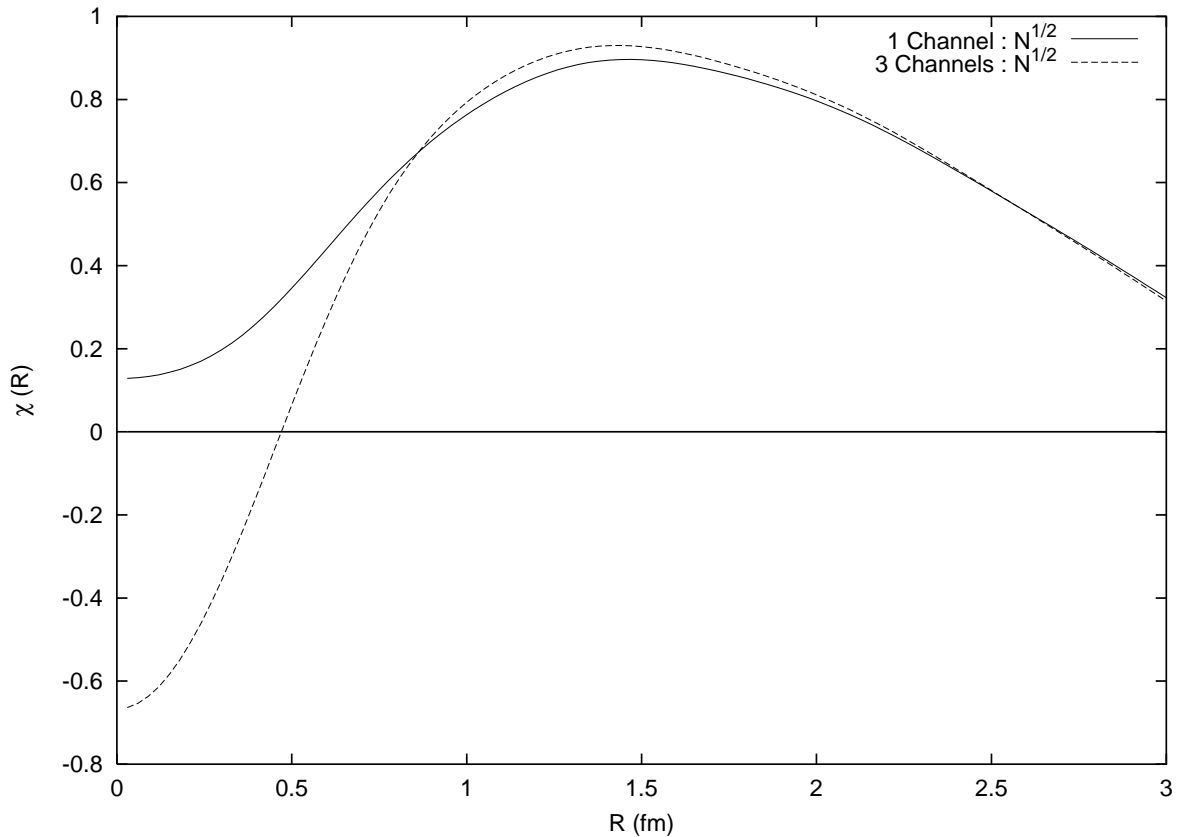


FIG. 3. The relative wave function of Eq. (5.3) for the 3S_1 partial wave for $k = 1 \text{ fm}^{-1}$ obtained in one channel (solid line) and three channels (dashed line) calculations.

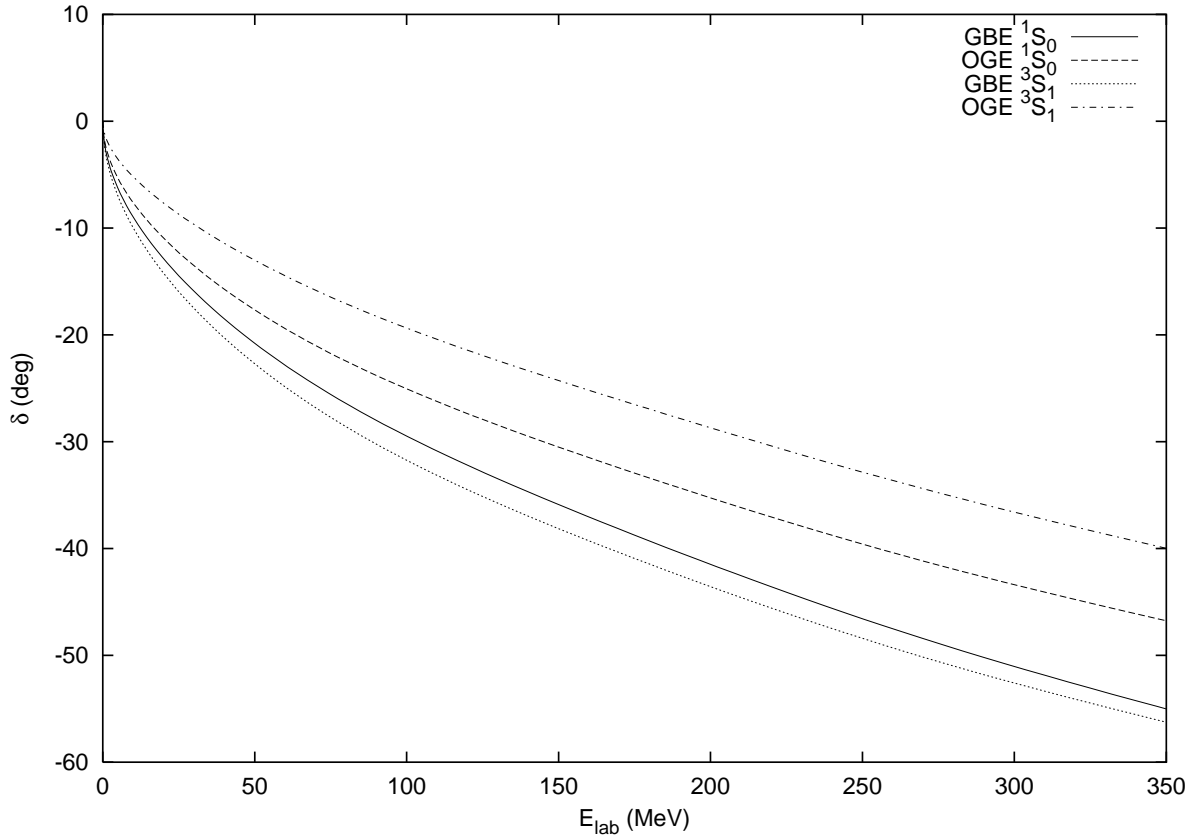


FIG. 4. 1S_0 and 3S_1 NN scattering phase shifts as a function of the laboratory energy E_{lab} .

The solid and dotted lines show the result corresponding to the GBE model and the dashed and dot-dashed lines that of the OGE model (see Ref. [31]).